Supporting Information to accompany

Imaging Disulfide Dinitroxides at 250 MHz to Monitor Thiol Redox Status

Hanan Elajaili, Joshua R. Biller, Gerald M. Rosen, Joseph P. Y. Kao, Mark Tseytlin, Laura A. Buchanan, George A. Rinard, Richard W. Quine, Joseph McPeak, Yilin Shi, Sandra S. Eaton, and Gareth R. Eaton *

EPR Linewidths

Table S1.[a]

Full widths at half height (G) for lines 1 and 2 in the absorption spectra of diradicals **I** and **II**, and line 1 of monoradicals **Ia** and **IIa**, as a function of observation frequency. Linewidths were determined by simulation as overlapping Lorentzians using locally written software or by measurement with the cursors in the Xepr software.

Diradical		**I**		**II**	
	Frequency	Line 1	Line 2	Line 1	Line 2
X	9.2 GHz	2.3	8.7	1.2	14.5
L	1.04 GHz	3.8	10	1.8	14.0
VHF	250 MHz	7.0	16	4.0	16.5
Monoradical		**Ia**		**IIa**	
		Line 1		Line 1	
X	9.2 GHz	1.5		0.6	
L	1.04 GHz	1.8		0.8	
VHF	250 MHz	1.6		0.8	

[a] Concentrations are 0.5 mM. Spectra were recorded in equilibrium with air. Uncertainties are ca. 5% for line 1 and 5 - 10% for the exchange-broadened line 2. Lines are numbered from low-field to high-field.

*Relaxation Times for **I**, **Ia**, **II** and **IIa** at X-band*

The broader lines for diradicals **I** and **II** than for monoradicals **Ia** and **IIa** (Table S1) are attributed to faster relaxation rates. To confirm this assignment relaxation times were examined. Progressive power saturation for the low-field lines (line 1) in deoxygenated samples showed that the curve for monoradical **Ia** deviates from linearity at lower power than for diradical **I** (Fig. S1), consistent with slower relaxation of the monoradical than of the diradical.

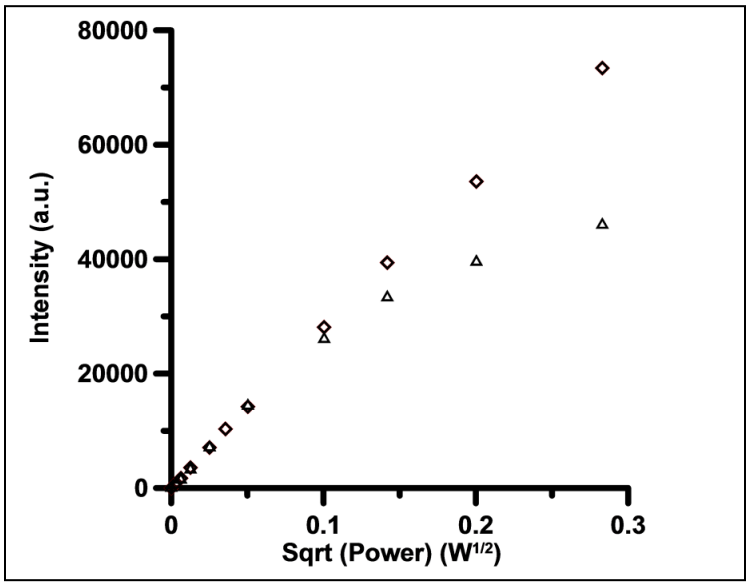

Figure S1. X-band power saturation curves for the low-field lines (line 1) of deoxygenated 0.5 mM aqueous solutions of **I** (◊) and of **Ia** (Δ) generated by reduction with 0.5 mM glutathione.

Solutions for pulsed EPR relaxation studies were placed in thin-walled Teflon tubing, supported in 4 mm OD quartz tubes. To remove oxygen, nitrogen gas was passed over the samples until there was no further change in relaxation time.

Relaxation times measured by two-pulse spin echo and inversion recovery in the presence and absence of O_2 are summarized in Table S2. Comparison values are included for the carboxy-proxyl (3-carboxy-2,2,5,5-tetramethyl-1-pyrrolidinyloxyl) radical [1]. For both T_1 and T_2 the values decrease in the order carboxy-proxyl > monoradical > diradical. For the carboxyl-proxyl radical in aqueous solution at 20^{o}C the tumbling correlation time, τ_R, is 19 ps, and at X-band modulation of the anisotropic nitrogen hyperfine interaction by molecular tumbling dominates T_1 [2]. The molar masses for the diradicals are about twice as large as for the monoradicals, so tumbling correlation times are about twice as long for the diradicals as for the monoradicals. Slowing tumbling would make T_1 longer at X-band if the dominant mechanism was the same as for carboxy-proxyl. The shorter values of T_1 for the diradicals than for the monoradicals suggests domination by a different mechanism which is proposed to be modulation of the dynamic exchange interaction. In the fast tumbling limit T_1 is the dominant contribution to T_2 and so $T_2 \sim T_1$. As tumbling slows, incomplete motional averaging of g and A anisotropy makes increasing contributions and T_2 decreases. Thus the shorter values of T_2 for the diradicals than for the monoradicals are consistent with increased contributions from incomplete motional averaging.

The relaxation times for the exchange broadened lines (lines 2 and 4 for **I** and line 3 for **II**) are too short to be measured directly on available instrumentation.

Table S2.

T_1 and T_2 values (in μs) at X-band for 0.5mM aqueous solutions.[a]

A. T_1 [a]

		T_1 (N_2)	T_1 (air)
^{14}N	I	0.43	0.36
	Ia	0.52	0.43
	proxyl[b]	0.72	
^{15}N	II	0.51	0.34
	IIa	0.86	0.52
	proxyl[b]	1.0	

[a] Relaxation times are the average for lines 1, 3, and 5 for ^{14}N, or lines 1 and 3 for ^{15}N, measured with 40 ns 90° pulses.

[b] Values from [1]

B. T_2[a]

		T_2 (N_2)	T_2 (air)
^{14}N	I	0.14	0.12
	Ia	0.25	0.22
	proxyl[b]	0.57	
^{15}N	II	0.29	0.21
	IIa	0.42	0.25
	proxyl[b]	0.75	

[a] Relaxation times are the average for lines 1, 3, and 5 for ^{14}N, or lines 1 and 3 for ^{15}N, measured with 40 ns 90° pulses. Uncertainties are 5 – 10%

[b] Values from [1]

The exchange-broadened lines for **I** (lines 2 and 4 in Fig. 2) have such short T_2 that an echo is not observed for these lines in buffer solution at ambient conditions (Fig. S2). The high-field line (line 5) has shorter T_2 than the low-field and center-field lines (Fig. S2) due to incomplete averaging of g and A anisotropy.

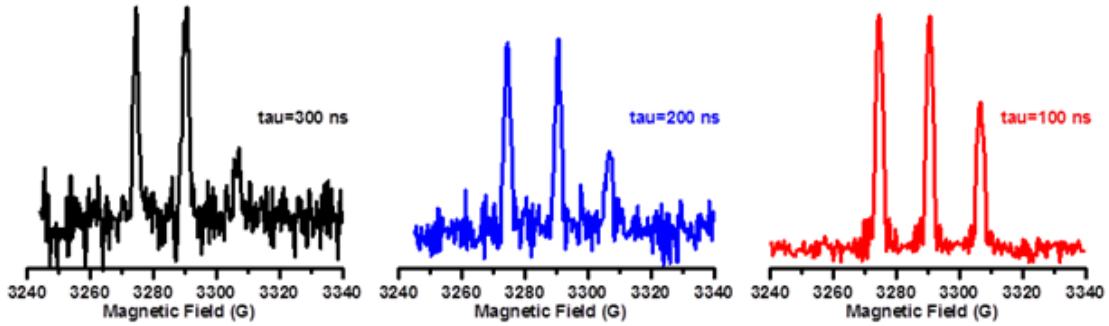

Figure S2. Field-swept echo-detected spectra of diradical **I** at X-band. The relaxation times for peaks 2 and 4 are so short that echoes are not detected at these tau values. As the time tau between pulses of the 2-pulse sequence is increased, the relative intensity of the echo for line 5 decreases because of the shorter T_2.

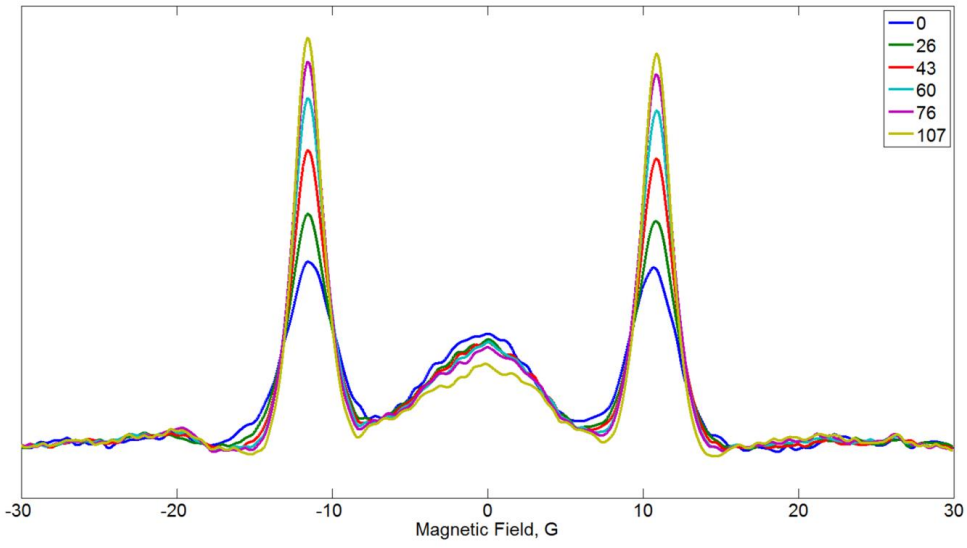

Figure S3. Time dependence of slices through the lower compartment of the image shown in Figure 8, showing the changes in lineshape as **II** is cleaved by reaction with glutathione to form **IIa**.

Diradical **III**

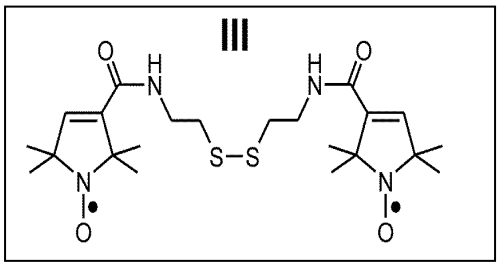

The large linewidths for lines 2 and 3 in the spectra of **I**, reduce the amplitudes of the characteristic lines for the diradical and make them more difficult to image. Those lines would be sharper if the exchange interaction were stronger. To determine whether replacing the saturated nitroxide ring of **I** with an unsaturated nitroxide ring, diradical **III** [3] was examined. The X-band spectrum for 0.12 mM **III** in water plus a small amount of DMSO is shown in Figure S4, along with the spectrum of **I**. The linewidths for peaks 2 and 4 in the spectrum of **III** are somewhat narrower than for **I** (Fig. S4), which indicates stronger exchange interaction. Thus the additional double bond in the rings of **III** increases the spin-spin interaction slightly. This may be due to more extensive delocalization of the unpaired electrons which enhances the effectiveness of the exchange interaction during intramolecular collisions on the nitroxide moieties. The differences in linewidths between the saturated and unsaturated nitroxide rings of **I** and **III** are not large enough to strongly favor either radical for imaging redox state.

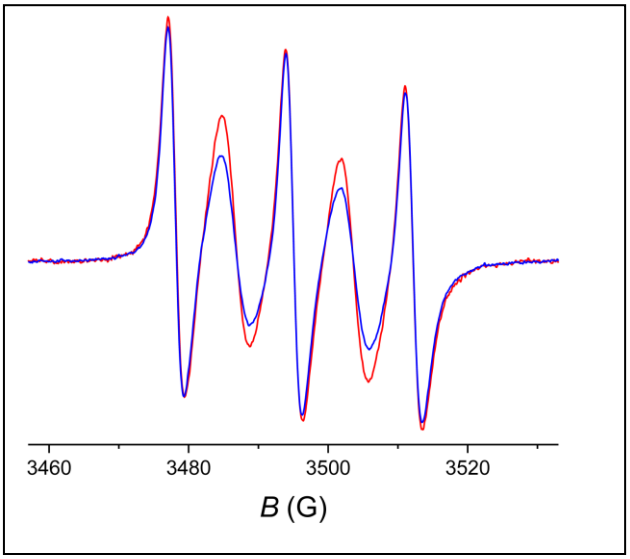

Figure S4. X-band CW spectra of **I** (blue) and **III** (red).

References

[1] J.R. Biller, V. Meyer, H. Elajaili, G.M. Rosen, J.P.Y. Kao, S.S. Eaton, and G.R. Eaton, Relaxation Times and Line Widths of Isotopically-Substituted Nitroxides in Aqueous Solution at X-band. J. Magn. Reson. 212 (2011) 370-377.

[2] J.R. Biller, H. Elajaili, V. Meyer, G.M. Rosen, S.S. Eaton, and G.R. Eaton, Electron Spin Lattice Relaxation Mechanisms of Rapidly-Tumbling Nitroxide Radicals. J. Magn. Reson. 236 (2013) 47 - 56.

[3] E.A. Legenzov, S.J. Sims, N.D.A. Dirda, G.M. Rosen, and J.P.Y. Kao, Disulfide-linked dinitroxides for monitoring cellular thiol redox status through electron paramagnetic resonance spectroscopy Biochemistry submitted for publication (2015).